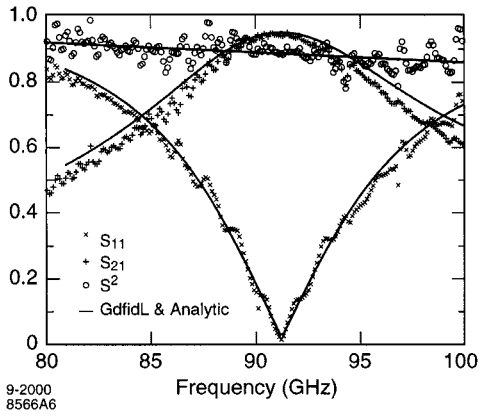

Fig. 2. Plot of measured scattering parameters S_{11} and calculated scattering parameters for a sample window ($S^2 = S_{11}^2 + S_{21}^2$).

with the foregoing, while they have all passed a leak check. Thus far, we have seen no evidence of breakdown, multipactor, fracture, or puncture, even while realizing that such phenomena are part of the experiment, and part of the utility of the apparatus in the first place.

IV. Conclusions

We have begun to develop vacuum-compatible components in WR10 for operation with a miniature accelerator. The immediate and initial purpose for the window was to permit monitoring of power developed in a subharmonic interaction circuit. Alternatives to a window include coaxial feedthrough, horn output through a window, taper to oversize guide, and window. However, all of these techniques have their own challenges and, even if successful, leave one with a more complicated power calibration. More than that, they are not ideally suited for accelerator component development. With a WR10 window, we can couple power to other WR10 components in a straightforward way. We expect that development of more sophisticated quasi-optical accelerator components will later benefit from the calibrations and other work facilitated by this simple, yet robust, window design.

Acknowledgment

The authors wish to acknowledge the support and encouragement of G. Caryotakis, Stanford Linear Accelerator Center (SLAC), Stanford University, Stanford, CA, and J. Huth, Harvard University, Cambridge, MA, helpful conversations with W. R. Fowkes, SLAC, Stanford University, Stanford, CA, and the expert assistance of D. Miller, SLAC, Stanford University, Stanford, CA, and D. Millican, SLAC, Stanford University, Stanford, CA.

References

[1] G. Caryotakis, "High power microwave tubes: In the laboratory and on-line," *IEEE Trans. Plasma Sci.*, vol. 22, pp. 683–691, Oct. 1994.

[2] D. H. Whittum, "Ultimate gradient in solid-state accelerators," in *Proc. Adv. Accelerator Concepts Workshop*.

[3] R. H. Siemann. W-band vector network analyzer based on an audio lock-in amplifier. *Phys. Rev.*, unpublished.

[4] W. Bruns, "$GdfidL$: A finite difference program for arbitrarily small perturbations in rectangular geometries," *IEEE Trans. Magn.*, vol. 32, pp. 1453–1456, May 1996.

A Technique for Determining the Normalized Impedance of Slots in the Image Plane of the Image NRDG

Lawrence C. Chirwa, Manabu Yamamoto, Manabu Omiya, and Kiyohiko Itoh

***Abstract*—This paper presents a method for determining the normalized impedance of a transverse slot in the image plane of the image nonradiative dielectric guide using measurements of the standing wave. The method overcomes the problem of distortion caused by the scattered evanescent fields that are present in the vicinity of the slot. The measurement equipment, its optimum parameters, and aspects necessary for accurate measurements are also discussed. Moreover, the finite-difference time-domain technique is employed to determine the normalized slot impedance, and good agreement is obtained with measured results, confirming the reliability of the method.**

***Index Terms*—FDTD technique, image NRD guide, measurement of standing wave, millimeter-wave, normalized impedance, slot in the image plain.**

I. Introduction

Low insertion loss is one of the important properties that millimeter waveguides should have. The nonradiative dielectric waveguide (NRDG) [1] is one of the waveguides that posses this characteristic. The image nonradiative dielectric waveguide (iNRDG) [2], [3] is derived from the normal NRDG, and it has low insertion loss, very much like that of the normal NRDG from which it is derived. However, it has the advantage over the normal NRDG of being smaller in size.

The principle operation mode of the iNRDG is the lowest LSM mode, the LSM_{10} mode. As the LSM_{10} mode of the iNRDG is similar to the TE_{10} mode for rectangular waveguides, the design method for waveguide slot array antennas proposed in [4] and [5] can be used to design an iNRDG slot array antenna consisting of transverse slot elements. In order to utilize this design method, the normalized impedance of the transverse slot in the image plane needs to be known.

In this paper, we propose a method for determining the normalized impedance of a transverse slot that utilizes experimental measurements of the standing wave in the waveguide and takes into consideration the distortion effects of the higher mode evanescent fields in the vicinity of the slot. The equipment for measuring the standing wave and the optimum parameters of the probe used to measure the standing wave are also described. The normalized impedance results obtained using the technique proposed in this paper are validated by comparing them to results obtained using finite-difference time-domain (FDTD) analysis [6].

II. Measurement of the Standing Wave

The necessity of taking precise measurements of the fields of the standing-wave profile in order to accurately estimate the normalized impedance of the slot cannot be over emphasized. From the relationships used to determine the reflection coefficient, it is apparent that it is especially important to make precise measurements of the standing wave when the standing wave ratio (SWR) is almost equal to one. In this

Manuscript received July 16, 1999; revised March 2, 2000. This work was supported by the Ministry of Education, Science, Sports, and Culture of Japan under Grant-in-Aid for Developmental Scientific Research (A) (2) 11355017.

The authors are with the Graduate School of Engineering, Hokkaido University, Sapporo 060-8628, Japan.

Publisher Item Identifier S 0018-9480(01)03311-7.

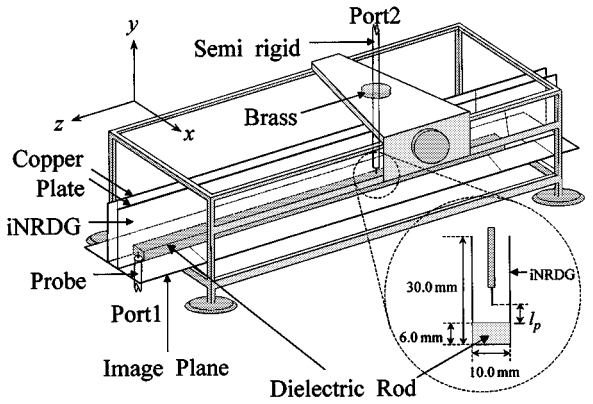

Fig. 1. Standing-wave measurement system for the iNRDG.

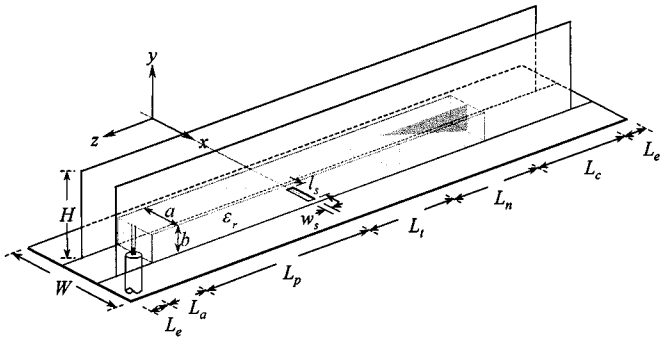

Fig. 2. iNRDG with a transverse slot in its image plane (used in experiments).

TABLE I
PARAMETERS OF THE EXPERIMENTAL iNRDG

ϵ_r	a	b	l_p	w_s	L_e	L_a
2.0	10.0	6.0	8.5	1.0	10.0	40.0

L_p	L_t	L_n	L_c	W	H
120.0	96.5	98.5	75.0	70.0	30.0

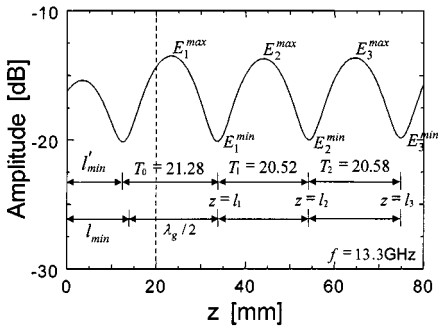

Fig. 3. Sample of the measured standing-wave distribution.

section, we describe in detail the standing-wave measurement equipment and measurement method, pointing out, in particular, those aspects necessary for accurate measurements.

Fig. 1 shows the rig used to measure the standing waves. The system is the same as that used for X-band standing wave measurements. To obtain the standing-wave distribution in the iNRDG, the detector is slid along the z-axis and measurements of $|S_{21}|$ between the feeding port (port 1) of the iNRDG and the measuring probe (port 2) are taken using the HP8510C network analyzer. The iNRDG is secured in the measurement rig in a manner such that the measuring probe moves along the z-axis parallel to the sidewalls and along the center of the dielectric strip. Moreover, it is ensured that the distance between the tip of the measuring probe and the dielectric surface is the same at all positions. The measuring probe is held firmly in position by a cylindrical brass fixer. The moving range of the probe is limited by the physical size of the measuring rig. In this case, the range was 108 mm. The distance along the z-axis was measured to an accuracy of 0.05 mm. However, this accuracy deteriorated to as large as 0.1 mm due to the backlash of the dial controlling the location of the probe.

The measuring probe length is chosen so that the probe has maximum sensitivity. The probe used was made from coaxial cable and can be regarded as a monopole element. Therefore, the probe has maximum sensitivity when its length is an odd multiple of $\lambda_o/4$, where λ_o is the wavelength in free space. In order to minimize disturbing the electromagnetic fields when carrying out measurements, a short probe length is desirable. As a result, a probe length of 5.35 mm was used. This corresponds to a quarter-wavelength at 14.0 GHz. The probe used was made from a thin coaxial cable with an inner conductor diameter of 0.49 mm. The probe was sharpened like a needle to minimize the error due to its finite width.

The current induced in the measuring probe is due to the y-component of the electric field. The electric field decays exponentially in the y-direction starting at the dielectric surface. Therefore, the distance from the dielectric to the tip of the probe, i.e., l_p, was chosen such that it was the maximum distance at which the measurements of the standing wave were within the dynamic range of the network analyzer. In this study, l_p was found to be 5.0 mm.

III. Evaluation of the Normalized Slot Impedance

In this section, we describe the technique used to accurately determine the normalized impedance of the slot from the measurement results of the standing wave, obtained as outlined in Section II. The technique does this by taking into consideration the distortion effects of the higher order modes scattered by the slot.

Fig. 2 shows the structure of the guide used and its parameters are presented in Table I. In this case, the dielectric material used was Teflon. The transverse slot is placed at a distance L_p from the coaxial probe that feeds the iNRDG. The nonreflective terminator is placed at a distance L_t in the direction opposite to the feeding probe from the slot. The terminator is made of resistive sheet (300 $\Omega/\square$) and is placed in the center of the dielectric in the y–z-plane at $x = a/2$ (shown in Fig. 2), as this is where the electric fields of the main mode have their maximum amplitude in the dielectric cross section. This terminator is similar to that used in the NRDG [7]. The length of the resistive sheet, i.e., L_n, is 98.5 mm, which corresponds to about $3\lambda_g$ at 14 GHz. As a result, the iNRDG of Fig. 2 behaves like an infinite guide in the $-z$-direction.

It is important that the quality of the terminating resistor (as regards to satisfying the matching condition) be very good in order to obtain accurate results. The quality of the terminator was verified by comparing the measured standing-wave distribution with that of an ideal iNRDG obtained using FDTD analysis. The FDTD problem space was terminated by perfectly matched layer (PML) absorbing boundary conditions (ABCs) that had a reflection at normal incidence of about only 2×10^{-4} (0.02%) [8].

Here, $z = 0$ is taken to be at the center of the slot and increases from the slot toward the feed. Fig. 3 shows the measured amplitude of the standing wave at 13.3 GHz from $z = 0$ mm to 80 mm. Measurements were taken at intervals of 0.5 mm. It is apparent from Fig. 3 that the maximum value at $z < 20$ mm is different to that of the maximums at $z > 20$ mm. Moreover, the separation T_o between the first two

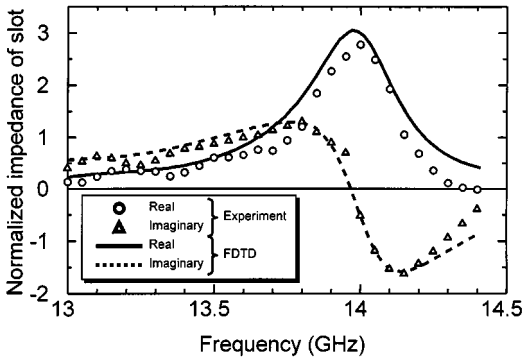

Fig. 4. Experimental and FDTD results of the normalized impedance of the slot.

minimum points nearest the slot is 21.28 mm, while the other separations between two minimum points ($T_1, T_2, \ldots$) are about 20.5 mm. These differences are attributed to the scattered higher order modes generated by the slot distorting the standing wave in the vicinity of the slot. Therefore, the normalized impedance should be calculated using standing-wave measurements that are taken some distance from the slot.

The maximums starting at the second maximum from the slot are denoted by $E_m^{\max}$, where $m = 1, 2, 3, \ldots$, as shown in Fig. 3. Similarly, the minimums starting at the second minimum from the slot are denoted by $E_m^{\min}$. The SWR is evaluated using the average value of these maximums and minimums using the expression

$$\mathrm{SWR} = \frac{\sum_{m=1}^{M_{\max}} E_m^{\max}/M_{\max}}{\sum_{m=1}^{M_{\min}} E_m^{\min}/M_{\min}} \tag{1}$$

where $M_{\max}$ and $M_{\min}$ are the total number of maximum and minimum values used, respectively. The values of $E_m^{\max}$ and $E_m^{\min}$ used in (1) are in their linear form. If the locations of $E_m^{\min}$ measured from the center of the slot are correspondingly denoted by l_m, then the wavelength in the iNRDG is evaluated as

$$\lambda_g = \frac{2\sum_{m=1}^{M_{\min}-1} (l_{m+1} - l_m)}{M_{\min} - 1}. \tag{2}$$

We let the distance between the center of the slot and the first minimum point be $l_{\min}$ in the ideal case where no higher order modes are generated by the slot. Considering that the period of the standing wave is $\lambda_g/2$, $l_{\min}$ is obtained from

$$l_{\min} = l_1 - \lambda_g/2. \tag{3}$$

In this case, the reflection coefficient Γ at the slot is determined using the SWR λ_g and $l_{\min}$, as in [9]. Since the transverse slot in the iNRDG is represented as a series impedance in the equivalent circuit, the normalized impedance is readily evaluated from the circuit as

$$z = \frac{2\Gamma}{1 - \Gamma}. \tag{4}$$

IV. Experimental and FDTD Results

The standing waves are measured over the frequency range from 13.0 to 14.4 GHz. Fig. 4 shows the normalized impedance of the slot evaluated using the technique outlined in this paper and the FDTD analysis. The slot of both the experimental guide and FDTD model were 8.5-mm long, 1-mm wide, and 1-mm thick. FDTD analysis was carried out on the ideal form of the iNRDG. This was achieved by placing PML ABCs [8] at all boundaries of the FDTD problem space. A transparent electric wall was used as the source and was in the form of a Gaussian pulse. It is seen from Fig. 4 that the resonant frequency is 14.0 GHz. The FDTD results were found to be in good agreement with experimental results.

V. Conclusion

This paper has presented a method of experimentally evaluating the normalized impedance of the transverse slot in the image plane of the iNRDG utilizing the standing-wave distribution in the waveguide. The method gives an accurate estimation of the normalized impedance regardless of the effects of the higher order modes generated in the vicinity of the slot due to scattering. This is achieved by an extrapolation method that utilizes measurement data at a distance from the slot that is not affected by the scattered fields. The optimum probe parameters and measurement configuration have also been presented. When the measured results are compared with FDTD analysis results, they are found to be in good agreement, confirming the effectiveness of the method. This technique may also find application in the determination of impedances, other than those of slots, in certain millimeter-wave devices.

References

[1] T. Yoneyama and S. Nishida, "Nonradiative dielectric waveguide for millimeter–wave integrated circuits," *IEEE Trans. Microwave Theory Tech.*, vol. MTT-29, pp. 1188–1192, Nov. 1981.

[2] Y. Sugawara, N. Nakaminami, N. Ishii, and K. Itoh, "A proposal of image NRD waveguide and radiation from its end," *Trans. Inst. Electron. Inf. Commun. Eng. B*, vol. J82-B, no. 4, pp. 637–644, Apr. 1999.

[3] T. Kikuma, N. Ishii, and K. Itoh, "A probe excitation for dielectric image line," *Trans. Inst. Electron. Inf. Commun. Eng. C*, pt. I, vol. J82-C-I, no. 4, pp. 219–225, Apr. 1999.

[4] S. Silver, Ed., *Microwave Antenna Theory and Design*. Stevenage, U.K.: Peregrinus, 1993.

[5] R. S. Elliott, *Antenna Theory and Design*. Englewood Cliffs, NJ: Prentice-Hall, 1981.

[6] K. S. Yee, "Numerical solution of initial boundary value problems involving Maxwell's equations in isotropic media," *IEEE Trans. Antennas Propagat.*, vol. AP-14, pp. 1327–1333, May 1966.

[7] T. Yomeyama, "Millimeter wave integrated circuits using nonradiative dielectric waveguide," *Trans. Inst. Electron. Inf. Commun. Eng. C*, pt. I, vol. J73-C-I, no. 3, pp. 87–94, Mar. 1990.

[8] D. M. Pozar, *Microwave Engineering*, 2nd ed. New York: McGraw-Hill, 1998.

[9] J. P. Berenger, "A perfectly matched layer for the absorption of electromagnetic waves," *J. Comput. Phys.*, vol. 114, no. 1, pp. 185–200, Jan. 1994.